

Weighted curvature approximation: numerical tests for 2D dielectric surfaces

Charles-Antoine Guérin, Gabriel Soriano and Tanos Elfouhaily

Institut Fresnel, UMR CNRS 6133, Faculté des Sciences de Saint-Jérôme, case 162,
F-13397 Marseille Cedex 20, France

Received 26 November 2003

Published 19 May 2004

Online at stacks.iop.org/WRM/14/349

DOI: 10.1088/0959-7174/14/3/009

Abstract

The weighted curvature approximation (WCA) was recently introduced by Elfouhaily *et al* [7] as a unifying scattering theory that reproduces formally both the tangent-plane and the small-perturbation model in the appropriate limits, and is structurally identical to the former approximation with some different slope-dependent kernel. Due to the simplicity of its formulation, the WCA is interesting from a numerical point of view and the aim of the present paper is to establish its accuracy on some representative test cases. We derive statistical formulae for the coherent field and the cross-section in the case of stationary Gaussian random surfaces. We then specialize to the case of isotropic Gaussian spectra and perform numerical comparisons against rigorous method of moments (MoM)-based results on 2D dielectric surfaces. We show that the WCA remains extremely accurate in a roughness range where other first-order classical approximations (small-slope and Kirchhoff) clearly fail, at the same computational cost.

(Some figures in this article are in colour only in the electronic version)

1. Introduction

Despite the evolution of computer capacities, the rigorous numerical computation of scattering by random rough surfaces remains too demanding, especially when it comes to Monte Carlo averages or large samples. Therefore simple old approximations such as the small-perturbation method (SPM) and the Kirchhoff approximation (KA) are still employed on a regular basis. Now, these methods have a limited domain of validity and are in principle accurate in the asymptotic high- or low-frequency regimes only (in terms of electromagnetic frequency). This is why there has been a constant effort in the literature in developing approximate methods that hold in the intermediate regime but also present a good compromise between numerical efficiency and accuracy. A suitable approximate method should meet the following requirements:

1. It must be *universal*, that is should not depend on or be restricted to a simplified scattering problem: 1D surfaces, Dirichlet or Neumann scalar problem, acoustic case and perfect conductors. It should in fact be applicable to the full-vectorial 3D dielectric problem, in which case it can be easily specialized to the aforementioned problems.
2. It must respect some fundamental *a priori* physical properties of the scattering amplitude: (a) reciprocity, (b) shift invariance and (c) tilt invariance.
3. It should not be restricted to a high-frequency or low-frequency regime but should be able to cope with both limits. Therefore, it must be a unifying theory in that it reproduces the (a) small-perturbation method (SPM) and (b) the Kirchhoff approximation (KA) in the appropriate limits.
4. It must be numerically efficient, that is the computations must be (a) fast, (b) easy to implement and (c) reliable (no numerical instability).
5. It should give the scattering amplitude a simple analytical expression that makes the dependence upon the surface parameters explicit, and allows for qualitative prediction.
6. It should provide analytical statistical expressions (at least for Gaussian surfaces) for the scattering cross-section, in order to avoid Monte Carlo procedures.
7. It should account for cross-polarization, especially in the incidence plane.
8. Its accuracy should not be sensitive to the incidence or scattering (non-grazing) angles, nor to the polarization.
9. It should have the widest possible validity domain in terms of surface parameters outside the SPM and KA regimes.

Among the large number of approximate methods that have been developed in the last two decades, we dare think none of them can be recognized to fulfil all these requirements. We would not review here the existing methods but will only mention some of the best candidates with respect to our criteria of evaluation. The first one is the small-slope approximation (SSA) of Voronovich [24–26]. At first order (SSA-1) it satisfies items 1, 2-ab, 3-a, 4-abc, 5, 6. At second order (SSA-2), it gains 2-abc, 3-ab, 7 but loses 4-abc. The second candidate is the operator expansion method (OEM) of Milder [12–14, 17]. At first order (OEM-1), it already possesses 1,2-ab, 3ab, 4-ac, 7. The point 2-c has not been investigated and the omission of item 4-b is a subjective appreciation (we found the method presented in [17] extremely complex). The main weakness of the OEM is the absence of statistical formulation. The local weight approximation (LWA) of Dashen and Wurmser [4–6] satisfies 2-abc, 3, 4, 5 but misses the essential item 1. For these three methods, one cannot give a definitive answer to items 8, 9 due to the lack of numerical experiments.

In this paper we would like to test a method which was recently introduced by Elfouhaily *et al* [7], namely the weighted curvature approximation (WCA), which retains features from both SSA and LWA. By construction it satisfies 1, 2-abc, 3, 4, 5 and we would like to investigate items 6–9 to see if it is a worthy candidate to complement the aforementioned methods.

2. Geometry and notations of the scattering problem

2.1. Surface geometry

A rough surface Σ separates the vacuum (upper medium) from a homogeneous dielectric medium (lower medium). We chose the right Cartesian coordinate $(\hat{\mathbf{x}}, \hat{\mathbf{y}}, \hat{\mathbf{z}})$ system with z -axis directed upwards and assume Σ is given by a Cartesian equation $z = h(\mathbf{r}) = h(x, y)$, where h is assumed to be the realization of a random stationary process. For an arbitrary vector \mathbf{a} , the notation a will refer to its norm and $\hat{\mathbf{a}}$ to its direction. A downward propagating electromagnetic plane wave with wave vector $\mathbf{K}_0 = (k_0, -q_0)$ and wavenumber $K = 2\pi/\lambda$ is incident on

the surface and gives rise to up-going scattered wave vectors in directions $\mathbf{K} = (\mathbf{k}, q_k)$. The vectors \mathbf{k}_0 and \mathbf{k} are the horizontal components of the incident and scattered waves, respectively, and q_0, q_k are the vertical (positive) components. They are related by the relation $k^2 + q_k^2 = k_0^2 + q_0^2 = K^2$. The vector $\mathbf{Q} = \mathbf{K} - \mathbf{K}_0$ is the so-called momentum transfer [16] and plays an important role in scattering theory. We will denote by $\mathbf{Q}_H = \mathbf{k} - \mathbf{k}_0$ and $Q_z = q_0 + q_k$ its horizontal and vertical components, respectively. The incident and scattered fields are decomposed over the fundamental polarization basis.

$$\mathbf{p}_{\pm 1}^{\pm}(\mathbf{k}) = \frac{k\hat{\mathbf{z}} \mp q_k\hat{\mathbf{k}}}{K}, \quad \mathbf{p}_{\pm 2}^{\pm}(\mathbf{k}) = \hat{\mathbf{z}} \times \hat{\mathbf{k}}.$$

The case \mathbf{p}_1^{\pm} corresponds to the vertical polarization (V-polarization), where the electric field lies in the $(\hat{\mathbf{z}}, \hat{\mathbf{k}})$ plane; \mathbf{p}_2^{\pm} is the horizontal polarization (H-polarization), with an electric field in the horizontal plane $(\hat{\mathbf{x}}, \hat{\mathbf{y}})$. The minus superscript corresponds to down-going plane waves while the plus superscript refers to the up-going waves. The scattering operator $\mathbb{S}(\mathbf{k}, \mathbf{k}_0)$ relates the incident and scattered waves. In dyadic notation it can be written as

$$\mathbb{S}(\mathbf{k}, \mathbf{k}_0) = \sum_{i,j=1}^2 S_{ji}(\mathbf{k}, \mathbf{k}_0) \mathbf{p}_j^+(\mathbf{k}) \mathbf{p}_i^-(\mathbf{k}_0). \quad (2.1)$$

The two-by-two matrix $\mathcal{S}(\mathbf{k}, \mathbf{k}_0) = (S_{ji})(\mathbf{k}, \mathbf{k}_0)$ is called the scattering matrix. For an incident wave with unit amplitude and pure i polarization,

$$\mathbf{E}_0(\mathbf{r}, z) = e^{i\mathbf{k}_0 \cdot \mathbf{r} - iq_0 z} \mathbf{p}_i^-(\mathbf{k}_0),$$

the scattered field above the surface writes is written as

$$\mathbf{E}_s(\mathbf{r}, z) = \frac{1}{q} \int d\mathbf{k} e^{i\mathbf{k} \cdot \mathbf{r} + iqz} \sum_{j=1,2} S_{ji}(\mathbf{k}, \mathbf{k}_0) \mathbf{p}_j^+(\mathbf{k}). \quad (2.2)$$

Our normalization of the scattering amplitude differs by a trivial geometrical factor of some other conventions. For instance, Voronovich uses a prefactor $\sqrt{q_0/q}$ instead of $1/q_0$ in the defining equation (2.2). The so-called mean reflection coefficient is related to the coherent part of the scattering matrix. For extended targets such as infinite rough surfaces, it is defined by

$$V(\mathbf{k}_0) = \lim_{\text{Area} \rightarrow \infty} \frac{\langle S_{ji}(\mathbf{k}_0, \mathbf{k}_0) \rangle}{\text{Area}}, \quad (2.3)$$

where Area is the illuminated area and the brackets $\langle \cdot \rangle$ stand for the ensemble average. The incoherent scattered normalized radar cross-section (NRCS) is related to the second moment of the scattering matrix.

$$\sigma_{ji}^0(\mathbf{k}, \mathbf{k}_0) = \lim_{\text{Area} \rightarrow \infty} \frac{4\pi^2 K \langle |S_{ji}(\mathbf{k}, \mathbf{k}_0) - \langle S_{ji}(\mathbf{k}, \mathbf{k}_0) \rangle|^2 \rangle}{q_0 \text{Area}}. \quad (2.4)$$

Some authors prefer to use the bistatic cross-section $2q_0\sigma_{ji}^0$.

3. A short review on approximate methods

Before introducing the WCA, we will briefly review the approximate models at which this method takes its roots.

3.1. The small-perturbation model

The small-perturbation model (SPM) is the oldest and still most employed approximate method in scattering from rough surface. It is based on a systematic expansion of the scattering amplitude in order of surface height. At first order, it involves merely the Fourier transform of roughness, while it implies a more complicated Fourier kernel at higher orders. In practice, the expansion is used at the lowest two orders only, the successive terms becoming intractable. The scattering matrix in the framework of SPM is given by

$$\mathbb{S}(\mathbf{k}, \mathbf{k}_0) = \frac{1}{Q_z} \mathbb{B}(\mathbf{k}, \mathbf{k}_0) [\delta(\mathbf{Q}_H) - iQ_z \widehat{h}(\mathbf{Q}_H)] - Q_z \int \mathbb{B}_2(\mathbf{k}, \mathbf{k}_0; \boldsymbol{\xi}) \widehat{h}(\mathbf{k} - \boldsymbol{\xi}) \widehat{h}(\boldsymbol{\xi} - \mathbf{k}_0) d\boldsymbol{\xi}, \quad (3.5)$$

where \widehat{h} is the Fourier transform of roughness:

$$\widehat{h}(\boldsymbol{\xi}) = \frac{1}{(2\pi)^2} \int e^{-i\boldsymbol{\xi}\cdot\mathbf{r}} h(\mathbf{r}) d\mathbf{r}.$$

The expression of the matrix $\mathcal{B}(\mathbf{k}, \mathbf{k}_0)$ is recalled in appendix A.

3.2. The Kirchhoff approximation

3.2.1. Low-frequency. The tangent plane and the low-frequency Kirchhoff approximation (KA-LF) are derived from the assumption that locally the surface can be considered flat compared to the incident radiation frequency. In this case, the Snell–Descartes law is applied in a local frame of reference to determine the electromagnetic surface current and therefore the radiated emergent field. This approximate model has the formal expression of an integral over a polarization integrand multiplied by some phase factors,

$$\mathbb{S}(\mathbf{k}, \mathbf{k}_0) = \frac{1}{Q_z} \int \mathbb{K}(\mathbf{k}, \mathbf{k}_0; -Q_z \nabla h) e^{-iQ_z h(\mathbf{r})} e^{-i\mathbf{Q}_H \cdot \mathbf{r}} \frac{d\mathbf{r}}{(2\pi)^2}, \quad (3.6)$$

where the polarization kernel is an explicit function of the local surface slopes ∇h . This dependence on the local slope is generally nonlinear and cannot be evaluated readily without further assumptions. However, when the surface is perfectly conducting, it can be shown (e.g., [9]) that the dependence is linear and the polarization integrand can be factored out after integration by part.

3.2.2. High-frequency. The high-frequency Kirchhoff approximation (KA-HF) is obtained in addition to the tangent plane derivation of (3.6) by the application of the stationary phase method in order to evaluate the polarization kernel at the critical points defined by the derivative of the phase. Under the high-frequency limit, the polarization kernel in (3.6) factors out, yielding

$$\mathbb{S}(\mathbf{k}, \mathbf{k}_0) = \frac{\mathbb{K}(\mathbf{k}, \mathbf{k}_0)}{Q_z} \int e^{-iQ_z h(\mathbf{r})} e^{-i\mathbf{Q}_H \cdot \mathbf{r}} \frac{d\mathbf{r}}{(2\pi)^2}, \quad (3.7)$$

where by definition $\mathbb{K}(\mathbf{k}, \mathbf{k}_0) = \mathbb{K}(\mathbf{k}, \mathbf{k}_0; \mathbf{Q}_H)$. The expression of the corresponding matrix $\mathcal{K}(\mathbf{k}, \mathbf{k}_0)$ in the canonical polarization basis is recalled in appendix A. In principle, the integral in the KA-HF (3.7) should be evaluated at the stationary or critical points. Hence the integral is replaced by a discrete sum which is the essence of the geometric optics limit. It is however more convenient to leave the integral form in (3.7) for further analytical and numerical developments. Under perfect conduction, the low- and high-frequency Kirchhoff models coincide for the reason invoked in the previous subsection.

The low- and high-frequency Kirchhoff models are very useful since they formally yield the geometric optics limit and fulfil some essential properties such as reciprocity, shift and tilt invariance. Unfortunately, these models do not reproduce another fundamental limit which is the SPM-1 limit. Intuitively, this deficiency is not surprising since the surface is considered locally flat and therefore no curvature corrections are present.

3.3. The small-slope approximation

Voronovich introduced in [26] a non-classical approach named the small-slope approximation (SSA). His model to first order (SSA-1) reads

$$\mathbb{S}(\mathbf{k}, \mathbf{k}_0) = \frac{\mathbb{B}(\mathbf{k}, \mathbf{k}_0)}{Q_z} \int e^{-iQ_z h(\mathbf{r})} e^{-iQ_H \cdot \mathbf{r}} \frac{d\mathbf{r}}{(2\pi)^2}, \quad (3.8)$$

which is essentially similar to KA-HF in (3.7) but with the polarization replaced by that of SPM-1 (see (3.5)). For this same reason, SSA-1 reproduces the SPM-1 limit but no longer the KA-HF limit (see [18]). The SSA to second order (SSA-2) is (see [25])

$$\mathbb{S}(\mathbf{k}, \mathbf{k}_0) = \frac{1}{Q_z} \int e^{-iQ_z h(\mathbf{r})} e^{-iQ_H \cdot \mathbf{r}} \frac{d\mathbf{r}}{(2\pi)^2} \left(\mathbb{B}(\mathbf{k}, \mathbf{k}_0) - iQ_z \int \mathbb{M}(\mathbf{k}, \mathbf{k}_0; \boldsymbol{\xi}) \hat{h}(\boldsymbol{\xi}) e^{i\boldsymbol{\xi} \cdot \mathbf{r}} d\boldsymbol{\xi} \right). \quad (3.9)$$

SSA-1 is now complemented by a double integral involving formally all derivatives of the surface through a Fourier kernel \mathbb{M} . This kernel is based on a combination of first- and second-order SPM kernels.

$$\mathbb{M}(\mathbf{k}, \mathbf{k}_0; \boldsymbol{\xi}) = \frac{1}{2} (\mathbb{B}_2(\mathbf{k}, \mathbf{k}_0; \mathbf{k} - \boldsymbol{\xi}) + \mathbb{B}_2(\mathbf{k}, \mathbf{k}_0; \mathbf{k}_0 + \boldsymbol{\xi}) - \mathbb{B}(\mathbf{k}, \mathbf{k}_0)). \quad (3.10)$$

This model is shown to have a second-order accuracy in surface slopes in [25]. Reciprocity, shift invariance, SPM-1 and SPM-2 limits are attained by construction. In a particular case of Dirichlet boundary condition, SSA-2 was shown in [25, 26] to reproduce the KA-HF limit. Recently, Guérin and Saillard [11] demonstrated that SSA-2 reproduces the KA-HF in the perfect conductor boundary conditions. Elfouhaily *et al* [8] noted some discrepancy in the general dielectric case. SSA-2 features tilt invariance up to linear order in the tilting vector according to Voronovich [27]. Since many fundamental limits are reached by SSA-2, it can be deemed analytically accurate although very cumbersome to implement numerically due to the complicated second-order kernel and some numerical instability which may arise in the evaluation of the double Fourier integral in (3.9). It would be more efficient to have same analytical accuracy but with a simpler functional form such as KA-LF. Direct evaluation of ensemble averaged quantities based on SSA-2 is not trivial and adds subtleties to an already complex model.

3.4. Dashen and Wurmser approach

Dashen and Wurmser [5] proved a theorem that an Ansatz based on a KA-LF structure can reach an accuracy up to the surface curvature:

$$\mathbb{S}(\mathbf{k}, \mathbf{k}_0) = \frac{1}{Q_z} \int \mathbb{G}(\mathbf{k}, \mathbf{k}_0; -Q_z \nabla h) e^{-iQ_z h(\mathbf{r})} e^{-iQ_H \cdot \mathbf{r}} \frac{d\mathbf{r}}{(2\pi)^2} + O\left(\frac{\nabla \nabla h}{K}\right)^2, \quad (3.11)$$

where the integrand is certainly dependent on the local surface slope as in KA-LF (3.6) but with a fundamentally different polarization kernel derived from formal compliance with tilt invariance. This tilt invariance imposed the following differential equation on the generic kernel to be solved analytically,

$$\mathbb{G}_0(\mathbf{k}, \mathbf{k}_0; \boldsymbol{\xi}) - \boldsymbol{\xi} \cdot \nabla \mathbb{G}_0(\mathbf{k}, \mathbf{k}_0; \boldsymbol{\xi}) = \hat{\mathbf{n}} \hat{\mathbf{n}}, \quad (3.12)$$

where $\hat{n} = (\mathbf{Q} - \boldsymbol{\xi})/\sqrt{Q^2 - 2\mathbf{Q} \cdot \boldsymbol{\xi} + \xi^2}$. The kernel \mathbb{G} and the corresponding scattering amplitude for the different boundary conditions (Dirichlet, Neumann and perfectly conducting case) are then simply expressed through this generic kernel. This model is named the local weight approximation (LWA) and satisfies most fundamental properties such as reciprocity, SPM-1 and KA-HF limit, as well as shift and tilt invariance. Since the kernel is solely derived from the differential equation in (3.12), Dashen and Wurmser's approach also gauges the importance of the tilt invariance property. Unfortunately, LWA does not exist for the general dielectric case because the differential equation in (3.12) turns intractable. The reason is that the right-hand side becomes heavily dependent on the dielectric constant of the rough surface.

4. The weighted curvature approximation

4.1. Construction of the WCA

Recently, Elfouhaily *et al* [7] derived a model named the weighted curvature approximation (WCA) based on KA-LF (3.6) or also the Dashen and Wurmser's (LWA) (3.11) Ansatz. They demonstrated that the integrand can be simply based on the SPM-1 polarization matrix, similar to SSA-1, along with a second-order correction involving the curvature kernel. This kernel is a simple difference between the low-frequency SPM-1 and KA-HF kernels expressed in a local frame of reference. The WCA takes the form

$$\mathbb{S}(\mathbf{k}, \mathbf{k}_0) = \frac{1}{Q_z} \int \{\mathbb{B}(\mathbf{k}, \mathbf{k}_0) - \mathbb{T}(\mathbf{k}, \mathbf{k}_0; -Q_z \nabla h)\} e^{-iQ_z h(\mathbf{r})} e^{-i\mathbf{Q}_H \cdot \mathbf{r}} \frac{d\mathbf{r}}{(2\pi)^2}, \quad (4.13)$$

where

$$\mathbb{T}(\mathbf{k}, \mathbf{k}_0; \boldsymbol{\xi}) = \mathbb{B}(\tilde{\mathbf{k}}, \tilde{\mathbf{k}}_0) - \mathbb{K}(\tilde{\mathbf{k}}, \tilde{\mathbf{k}}_0) \quad (4.14)$$

and the local wave vectors are given by

$$\tilde{\mathbf{k}} = \frac{\mathbf{k} + \mathbf{k}_0 + \boldsymbol{\xi}}{2}, \quad \tilde{\mathbf{k}}_0 = \frac{\mathbf{k} + \mathbf{k}_0 - \boldsymbol{\xi}}{2}.$$

The curvature kernel has the following properties,

$$\mathbb{T}(\mathbf{k}, \mathbf{k}_0; \mathbf{0}) = 0 \quad (4.15a)$$

$$\nabla \mathbb{T}(\mathbf{k}, \mathbf{k}_0; \mathbf{0}) = 0 \quad (4.15b)$$

$$\mathbb{T}(\mathbf{k}, \mathbf{k}_0; \mathbf{Q}_H) = \mathbb{B}(\mathbf{k}, \mathbf{k}_0) - \mathbb{K}(\mathbf{k}, \mathbf{k}_0), \quad (4.15c)$$

which ensure that both the SPM-1 and KA-HF are formally reached in the appropriate limits. Furthermore, the WCA is shown to be tilt invariant up to the linear order in a , as it satisfies the differential equation:

$$\mathbb{B}(\tilde{\mathbf{k}}, \tilde{\mathbf{k}}_0) \doteq \mathbb{B}(\mathbf{k}, \mathbf{k}_0) - \mathbb{T}(\mathbf{k}, \mathbf{k}_0; -Q_z \mathbf{a}) + \tilde{\mathbf{q}}_H \cdot \nabla \mathbb{T}(\mathbf{k}, \mathbf{k}_0; -Q_z \mathbf{a}) + O(a^2). \quad (4.16)$$

The WCA is also manifestly reciprocal and shift invariant. In [8], it was demonstrated that the curvature orders as derived from SSA-2 or from the difference between SPM-1 and Kirchhoff are equivalent. It is therefore possible to attain second-order accuracy with a single integral, which is of considerable importance in numerical applications.

We would like to draw attention to a pitfall that may arise from the local dependence of the kernel \mathbb{T} . When extracting the different polarization coefficients S_{ji} , one has to account for the change of polarization for the local wave vectors involved in the definition of T . Precisely we have

$$\mathbb{T}_{ji}(\mathbf{k}, \mathbf{k}_0; -Q_z \nabla h) = \sum_{i', j'=1,2} \mathbf{p}_j^+(\mathbf{k}) \cdot \mathbf{p}_{j'}^+(\tilde{\mathbf{k}}) [\mathcal{B}_{j'i'}(\tilde{\mathbf{k}}, \tilde{\mathbf{k}}_0) - \mathcal{K}_{j'i'}(\tilde{\mathbf{k}}, \tilde{\mathbf{k}}_0)] p_{i'}^-(\tilde{\mathbf{k}}_0) \cdot p_i^-(\mathbf{k}_0). \quad (4.17)$$

5. Statistical formula for the WCA

A nice feature of the WCA is the simplicity of its statistical formulation. We will assume in the following that the surface is described by a random stationary centred Gaussian process with correlation function $\rho(\mathbf{r}) = \langle h(\mathbf{r})h(0) \rangle$ and variance $\rho_0 = \rho(\mathbf{0})$.

5.1. Coherent scattering matrix

Using the technique presented in appendix B, we obtain the following expression for the mean reflection coefficient (2.3):

$$V_{ji}(\mathbf{k}_0) = \frac{1}{(2\pi)^2} \frac{\mathcal{B}_{ji}^c(\mathbf{k}_0, \mathbf{k}_0)}{2q_0} \exp[-2q_0^2 \rho_0], \quad (5.18)$$

where

$$\mathcal{B}_{ji}^c(\mathbf{k}, \mathbf{k}_0) = \mathcal{B}_{ji}(\mathbf{k}, \mathbf{k}_0) - \int T_{ji}(\mathbf{k}, \mathbf{k}_0, -Q_z \mathbf{u}) P(\mathbf{u}) d\mathbf{u}. \quad (5.19)$$

Here we have introduced the PDF of surface slopes:

$$P(\mathbf{u}) = \frac{1}{2\pi \sqrt{s_x^2 s_y^2 - s_{xy}^2}} \exp\left(-\frac{s_x^2 u_y + s_y^2 u_x - 2s_{xy} u_x u_y}{2(s_x^2 s_y^2 - s_{xy}^2)}\right) \quad (5.20)$$

with

$$s_x^2 = \langle |\partial_x h|^2 \rangle, \quad s_y^2 = \langle |\partial_y h|^2 \rangle, \quad s_{xy} = \langle \partial_x h \partial_y h \rangle. \quad (5.21)$$

Quadratic approximation. A direct consequence of the properties of the curvature kernel in (4.15) is its quadratic behaviour to lowest order.

$$\mathbb{T}(\mathbf{k}, \mathbf{k}_0; \boldsymbol{\xi}) \approx \boldsymbol{\xi} \mathcal{A} \boldsymbol{\xi} + O(\boldsymbol{\xi}^3) \quad (5.22)$$

where the pure curvature \mathcal{A} tensor is defined as the second derivative of generalized curvature kernel \mathbb{T} as

$$\mathcal{A}_{ji}(\mathbf{k}, \mathbf{k}_0) = \frac{1}{2} \nabla \nabla T_{ji}(\mathbf{k}, \mathbf{k}_0; \boldsymbol{\xi})|_{\boldsymbol{\xi}=0}. \quad (5.23)$$

In this approximation one gets, using the results of appendix B,

$$\mathcal{B}_{ji}^c(\mathbf{k}, \mathbf{k}_0) = \mathcal{B}_{ji}(\mathbf{k}, \mathbf{k}_0) - Q_z^2 \text{Trace}[\mathcal{A}_{ji} \boldsymbol{\Sigma}], \quad (5.24)$$

where $\boldsymbol{\Sigma} = (s_x^2, s_{xy}^2; s_{xy}^2, s_y^2)$ is the covariance matrix of slopes. For the acoustical cases with Neumann and Dirichlet boundary conditions, we can demonstrate that the curvature kernel \mathcal{A} is the dyadic notation

$$\mathcal{A}(\mathbf{k}, \mathbf{k}_0) = \frac{1}{2} \left\{ 1 + \frac{1}{2} \left(\frac{\mathbf{k}_0 \mathbf{k}_0}{q_0 q_0} + \frac{\mathbf{k} \mathbf{k}}{q_k q_k} \right) \right\}. \quad (5.25)$$

It should be noted that this result is dimensionless and therefore does not depend on the incident frequency or wavenumber K .

Equation (5.18) with (5.24) is equally obtained by Voronovich [26] (p 139, equation (5.4.13)) and Rodriguez [16] (equations (43) and (44)) in the Dirichlet case. Milder [15] also found the same result by a direct derivation from the operator expansion to first order for both Dirichlet and Neumann cases in his equations (43) and (45), respectively.

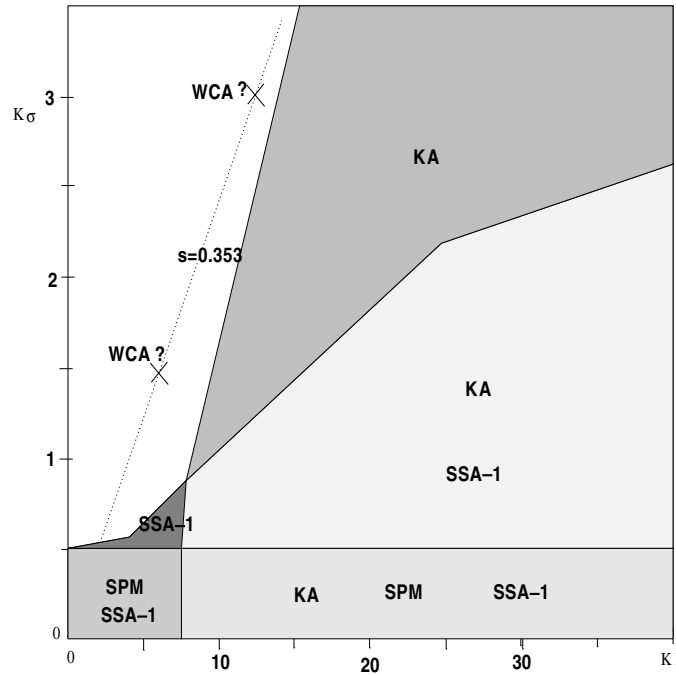


Figure 1. The validity domain of the different approximations.

5.2. Incoherent radar cross-section

The NRCS is easily obtained by use of the marginal generating function defined in appendix B,

$$\sigma_{ji}^0(\mathbf{k}, \mathbf{k}_0) = \frac{e^{-Q_z^2 \rho_0}}{Q_z^2} \int \{e^{Q_z^2 \rho(r)} |M_{ji}(\mathbf{k}, \mathbf{k}_0; \mathbf{r})|^2 - |\mathcal{B}_{ji}^c(\mathbf{k}, \mathbf{k}_0)|^2\} e^{-iQ_H \cdot \mathbf{r}} \frac{d\mathbf{r}}{(2\pi)^2}, \quad (5.26)$$

where

$$M_{ji}(\mathbf{k}, \mathbf{k}_0; \mathbf{r}) = \mathcal{B}_{ji}(\mathbf{k}, \mathbf{k}_0) - \int T_{ji}(\mathbf{k}, \mathbf{k}_0; -Q_z \mathbf{u} - iQ_z^2 \nabla \rho(\mathbf{r})) P(\mathbf{u}) d\mathbf{u} \quad (5.27)$$

or equivalently

$$M_{ji}(\mathbf{k}, \mathbf{k}_0; \mathbf{r}) = \mathcal{B}_{ji}(\mathbf{k}, \mathbf{k}_0) - \int T_{ji}(\mathbf{k}, \mathbf{k}_0; -Q_z \mathbf{u}) P(\mathbf{u} - iQ_z \nabla \rho(\mathbf{r})) d\mathbf{u}. \quad (5.28)$$

Isotropic surfaces. The formula (5.26) simplifies considerably in the case of an isotropic correlation function $\rho(\mathbf{r}) = \rho(r)$. Interchanging the order of integration between slope and position variable in (5.28) we easily obtain

$$\sigma_{ji}^0(\mathbf{k}, \mathbf{k}_0) = \sigma_{ji}^{(1)}(Q_H, Q_z) + \sigma_{ji}^{(2)}(Q_H, Q_z) + \sigma_{ji}^{(3)}(Q_H, Q_z). \quad (5.29)$$

The first term is the SSA-1 cross-section:

$$\sigma^{(1)}(Q_H, Q_z) = |\mathcal{B}_{ji}(\mathbf{k}, \mathbf{k}_0)|^2 e^{-Q_z^2 \rho_0} \int_0^\infty [e^{Q_z^2 \rho(r)} - 1] J_0(Q_H r) r \frac{dr}{2\pi}.$$

The second term is the cross-term between SSA1 and the WCA correction:

$$\sigma_{ji}^{(2)}(Q_H, Q_z) = -2\Re \left[\mathcal{B}_{ji}^*(\mathbf{k}, \mathbf{k}_0) \int d\mathbf{u} T_{ji}(\mathbf{k}, \mathbf{k}_0; -Q_z \mathbf{u}) P(\mathbf{u}) w_1(\mathbf{u}; Q_H, Q_z) \right]$$

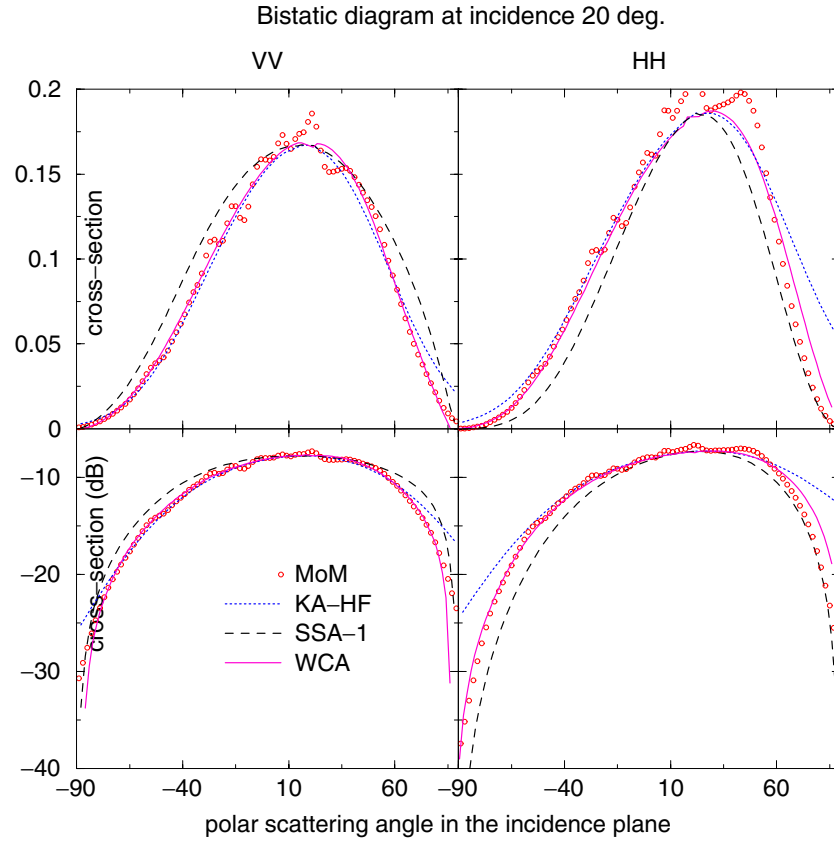


Figure 2. Bistatic diagram in the incidence plane for Gaussian isotropic correlation function with RMS height $\sigma = 0.25$ and correlation length $l = 1$ (in wavelength unit) at incidence $\theta_0 = 20^\circ$.

with

$$w_1(\mathbf{u}; Q_H, Q_z) = e^{-Q_z^2 \rho_0} \int_0^\infty e^{Q_z^2 \rho(r)} \left[e^{\frac{|Q_z \rho'(r)|^2}{2s^2}} J_0 \left(\left\| \mathbf{Q}_H - \frac{Q_z \rho'(r)}{r s^2} \mathbf{u} \right\| \right) - J_0(Q_H r) \right] r \frac{dr}{2\pi}$$

and $s^2 = s_x^2 = s_y^2 = -\rho''(0)$ and $s_{xy} = 0$. The third term is the quadratic term on the WCA correction:

$$\begin{aligned} \sigma_{ji}^{(3)}(Q_H, Q_z) &= \int d\mathbf{u}_1 d\mathbf{u}_2 T_{ji}(\mathbf{k}, \mathbf{k}_0; -Q_z \mathbf{u}_1) T_{ji}^*(\mathbf{k}, \mathbf{k}_0; -Q_z \mathbf{u}_2) \\ &\quad \times P(u_1) P(u_2) w_2(\mathbf{u}_1 - \mathbf{u}_2; Q_H, Q_z) \end{aligned}$$

or equivalently

$$\begin{aligned} \sigma_{ji}^{(3)}(Q_H, Q_z) &= \int d\mathbf{u}_1 w_2(\sqrt{2}\mathbf{u}_1; Q_H, Q_z) P(u_1) \\ &\quad \times \int d\mathbf{u}_2 P(u_2) T_{ji} \left(\mathbf{k}, \mathbf{k}_0; -Q_z \frac{\mathbf{u}_2 - \mathbf{u}_1}{\sqrt{2}} \right) T_{ji}^* \left(\mathbf{k}, \mathbf{k}_0; -Q_z \frac{\mathbf{u}_2 + \mathbf{u}_1}{\sqrt{2}} \right), \end{aligned}$$

with

$$w_2(\mathbf{u}; Q_H, Q_z) = e^{-Q_z^2 \rho_0} \int_0^\infty e^{Q_z^2 \rho(r)} \left[e^{\frac{|Q_z \rho'(r)|^2}{s^2}} J_0 \left(\left\| \mathbf{Q}_H - \frac{Q_z \rho'(r)}{r s^2} \mathbf{u} \right\| \right) - J_0(Q_H r) \right] r \frac{dr}{2\pi}.$$

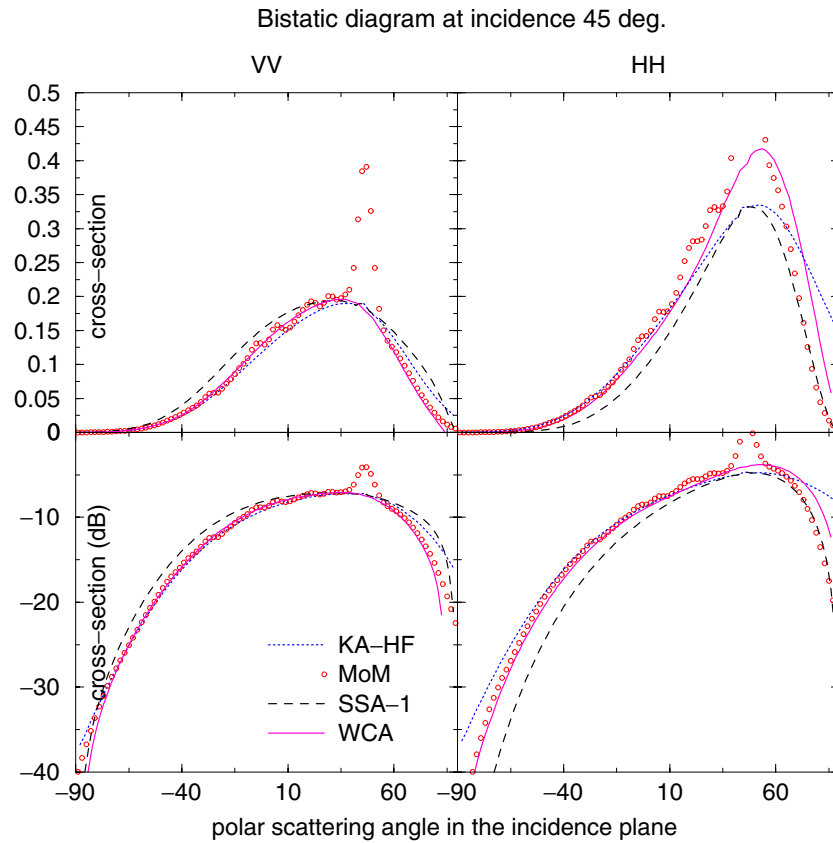


Figure 3. Same as figure 2 with $\sigma = 0.25$, $l = 1$, $\theta_0 = 45^\circ$.

Numerical efficiency. The kernel T_{ji} is a smoothly varying function and is exponentially attenuated by the p.d.f of slopes. Hence the multiple integrals over slope variables can be performed rapidly via a loose sampling over several RMS slopes. The most demanding part is the computation of the function w_1 and w_2 , which requires a tight sampling over several correlation lengths due to the oscillating nature of the integrand. Note that the second formulation of $\sigma_{ji}^{(3)}$ is more adapted to numerical computations since it involves the estimation of the function w_2 in one single loop over slopes. Altogether, the computational time is of the same order of magnitude as SSA-1.

6. Numerical trials

6.1. Test cases

The method has been numerically tested on 2D surfaces and compared with the method of moments (MoM) with an impedance approximation. We refer to [19, 20] for a complete presentation of the algorithmic of MoM and its numerical implementation for dielectric surfaces. Since no statistical formulation is available for the MoM, one has to resort to a Monte Carlo procedure on samples surfaces with a finite width of illumination. Due to the enormous amount of computational time that is required for 2D dielectric surfaces, we

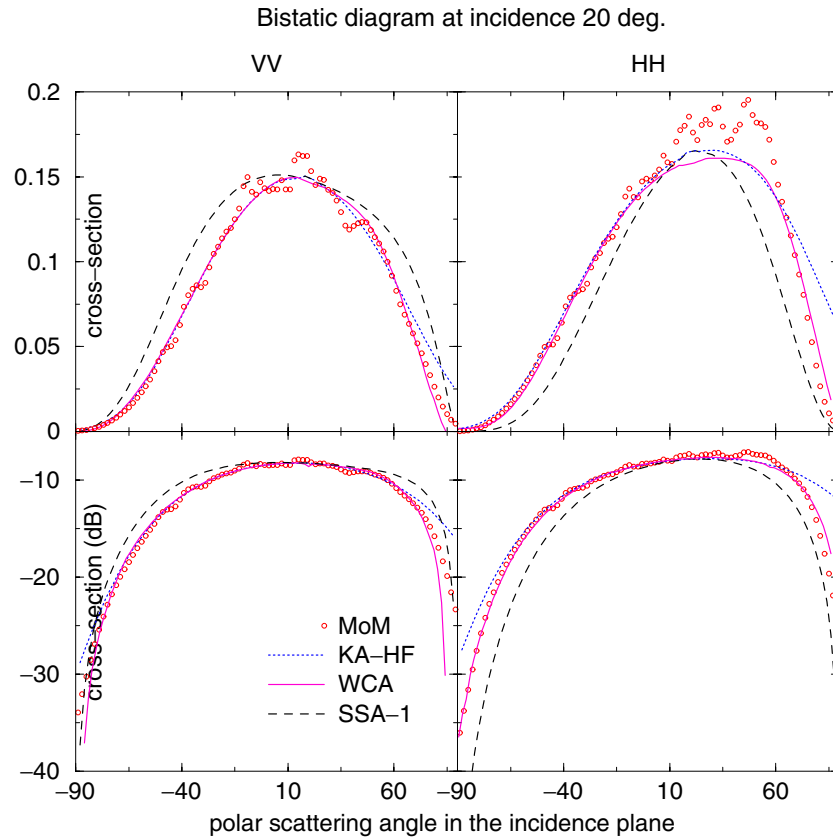


Figure 4. Same as figure 2 with $\sigma = 0.5$, $l = 2$, $\theta_0 = 20^\circ$.

restricted the study to single-scale surfaces with representative parameters, and limited the averaging procedure to about 400 samples. The test surfaces are Gaussian with isotropic Gaussian correlation function:

$$C(r) = \sigma^2 \exp(-r^2/l^2), \quad (6.30)$$

which can be considered as the paradigm of single-scale isotropic surfaces. The only two parameters are the RMS height σ and correlation length l . The RMS slope is given by $s^2 = 2\sigma^2/l^2$. The validity domain of KA and SSA-1 with respect to these parameters is by now well established (see [18] for 2D conducting surfaces or e.g. [2, 3, 21–23] for 1D surfaces). It is usually represented on a diagram with dimensionless parameters (Kl , $K\sigma$) (see figure 1). We will investigate a line of constant RMS slope $s = 0.353$, corresponding to a RMS angle of about 20° . There is an intermediate range on this line for which none of the usual approximations is valid. We will test the WCA for two points on this line: ($\sigma = 0.25$, $l = 1$) and ($\sigma = 0.5$, $l = 2$) (in wavelength unit).

6.2. Results

One intermediate value of permittivity corresponding to wet soils has been chosen ($\epsilon = 25 + 3i$) and two typical satellite incidences have been considered: $\theta_0 = 20^\circ$ and $\theta_0 = 45^\circ$. The bistatic diagrams have been presented in the incidence plane only, in both linear and logarithmic

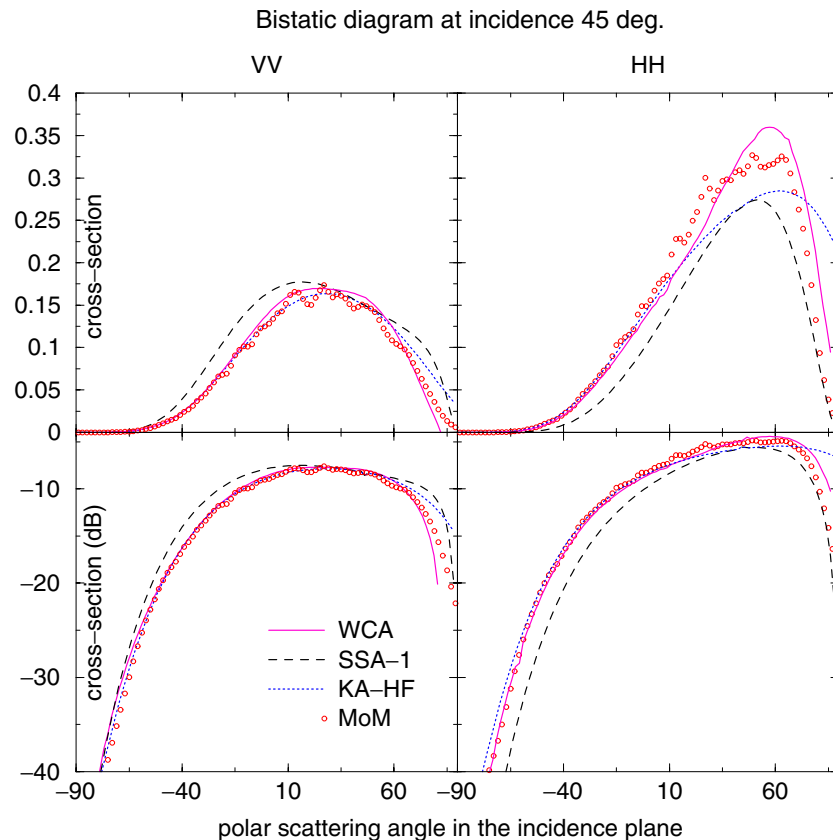


Figure 5. Same as figure 2 with $\sigma = 0.5$, $l = 2$, $\theta_0 = 45^\circ$.

scales, and for both co-polarizations (figures 2–5). For both roughness scales and incidences, the WCA appears to be superior by far to both KA-HF and SSA-1 and particularly accurate, except at forward grazing angles ($\theta \geq 75^\circ$) in HH polarization, where it, however, stays within 2.5 dB error. At backward grazing angles, it remains amazingly accurate in both polarizations. Surprisingly, the WCA performs even better at large roughness ($\sigma = 0.5$), where the contrast with the classical methods is striking. We also checked the cross-polarization coefficients, for which the WCA gave a bad estimate. This was expected since the WCA is a local theory which does not take multiple-scattering phenomena into account. We did not represent these coefficients to avoid making plots too difficult to read.

7. Conclusion

The WCA has been tested on some key cases which we think are typical of rough single-scale surfaces outside both the perturbative and high-frequency regimes. On these examples, one can clearly say that the WCA outperforms both KA and SPM and remains extremely accurate, thereby enlarging the validity domain of the former approximations. Hence we have given a positive answer to the points 6, 8, 9 mentioned in the introduction, the only negative but non-surprising result being the failure in cross-polarization. We are confident that the method will also perform well on multi-scale surfaces, but this has to be established.

Appendix A. Bragg and Kirchoff scattering matrices

The SPM-1 coefficients for dielectric boundary conditions are taken from the appendix of [27]

$$\begin{aligned}\mathcal{B}_{11}(\mathbf{k}, \mathbf{k}_0) &= \frac{2q_k q_0 (\epsilon - 1) (q'_k q'_0 \hat{\mathbf{k}} \cdot \hat{\mathbf{k}}_0 - \epsilon k k_0)}{(\epsilon q_k + q'_k)(\epsilon q_0 + q'_0)} \\ \mathcal{B}_{12}(\mathbf{k}, \mathbf{k}_0) &= \frac{2q_k q_0 (\epsilon - 1) K q'_k (\hat{\mathbf{k}} \times \hat{\mathbf{k}}_0) \cdot \hat{\mathbf{z}}}{(\epsilon q_k + q'_k)(q_0 + q'_0)} \\ \mathcal{B}_{21}(\mathbf{k}, \mathbf{k}_0) &= \frac{2q_k q_0 (\epsilon - 1) K q'_0 (\hat{\mathbf{k}}_0 \times \hat{\mathbf{k}}) \cdot \hat{\mathbf{z}}}{(q_k + q'_k)(\epsilon q_0 + q'_0)} \\ \mathcal{B}_{22}(\mathbf{k}, \mathbf{k}_0) &= -\frac{2q_k q_0 (\epsilon - 1) K^2 \hat{\mathbf{k}} \cdot \hat{\mathbf{k}}_0}{(q_k + q'_k)(q_0 + q'_0)}\end{aligned}$$

and the primed variables are defined as

$$q'_k = \sqrt{\epsilon K^2 - k^2} \quad (\text{A.1a})$$

$$q'_0 = \sqrt{\epsilon K^2 - k_0^2} \quad (\text{A.1b})$$

For simplicity, we use the Kirchoff matrix $\mathcal{K}(\mathbf{k}, \mathbf{k}_0)$ as simplified by [10, 1] and put in the following approximate form,

$$\mathcal{K}_{ji}(\mathbf{k}, \mathbf{k}_0) = \mathcal{R}_{ji}(Q/2) \mathcal{K}_{ji}^\infty(\mathbf{k}, \mathbf{k}_0), \quad (\text{A.2})$$

where \mathcal{K}^∞ is the Kirchoff matrix in the conducting case:

$$\mathcal{K}_{11}^\infty(\mathbf{k}, \mathbf{k}_0) = -\mathcal{K}_{22}^\infty(\mathbf{k}, \mathbf{k}_0) = [(K^2 + q_k q_0) \hat{\mathbf{k}} \cdot \hat{\mathbf{k}}_0 - k k_0]$$

$$\mathcal{K}_{12}^\infty(\mathbf{k}, \mathbf{k}_0) = -\mathcal{K}_{21}^\infty(\mathbf{k}, \mathbf{k}_0) = K(q_k + q_0) (\hat{\mathbf{k}} \times \hat{\mathbf{k}}_0) \cdot \hat{\mathbf{z}}$$

and the \mathcal{R} matrix is based on the Fresnel coefficients:

$$\mathcal{R}_{11}(q) = \frac{\epsilon q - \sqrt{(\epsilon - 1)K^2 + q^2}}{\epsilon q + \sqrt{(\epsilon - 1)K^2 + q^2}} \quad (\text{A.3a})$$

$$\mathcal{R}_{12}(q) = \mathcal{R}_{21}(q) = \frac{R_{11} + R_{22}}{2} \quad (\text{A.3b})$$

$$\mathcal{R}_{22}(q) = -\frac{q - \sqrt{(\epsilon - 1)K^2 + q^2}}{q + \sqrt{(\epsilon - 1)K^2 + q^2}}, \quad (\text{A.3c})$$

where ϵ is the relative permittivity. We recall that the variable Q is the norm of the momentum transfer $Q = |\mathbf{K} - \mathbf{K}_0| = \sqrt{Q_H^2 + Q_z^2}$.

This approximate Kirchoff model is valid for good conducting surfaces and away from grazing angles where $(\mathcal{R}_{11} - \mathcal{R}_{22})$ is assumed to be small.

Appendix B. A marginal generating function

Let $X = (x_1, x_2, \dots, x_N)$ be an N -dimensional Gaussian processes with the probability density function

$$P(X) = \frac{1}{(2\pi)^{N/2} \sqrt{|M|}} \exp \left[-\frac{1}{2} X \cdot M^{-1} \cdot X \right], \quad (\text{B.1})$$

where M is the covariance matrix $M_{ji} = \langle x_i x_j \rangle$. We define the marginal generating function (MGF) with respect to the process x_i as

$$G(X_{(-i)}; q) = \int P(X) e^{-iqx_i} dx_i. \quad (\text{B.2})$$

We bring the reader's attention to the fact that the previous integral is defined with respect to the process x_i and hence the result is a function of $N - 1$ remaining processes ($X_{(-i)}$) along with the dummy Fourier variable q . After some algebraic manipulations one finds a compact expression for the MGF as

$$G(X_{(-i)}; q) = \exp\left[-\frac{q^2}{2}M_{ii}\right] P(X - m)_{(-i)} \quad (\text{B.3})$$

where m is an effective mean vector of $N - 1$ dimensions and defined through its elements $m_j = -iqM_{ji}$. The subscript $(-i)$ in all previous equations refers to the omission of the i th random process and therefore turning the N -dimensional variable X into $X_{(-i)}$ with $N - 1$ dimensions.

A direct application of this simple MGF expression is when we evaluate the ensemble averaged scattering amplitude. The random Gaussian processes are now the surface elevation or a combination thereof with surface slopes. As an example, we have for the first process the difference between two surface elevations $x_1 = h_1 - h_2$ followed by the surfaced slopes ∇h , and hence the corresponding MGF is

$$\begin{aligned} G(\nabla h; Q_z) &= \int P(h_1 - h_2, \nabla h) e^{-iQ_z(h_1 - h_2)} d(h_1 - h_2) \\ &= \exp[-Q_z^2(\rho_0 - \rho)] P(\nabla h + iQ_z \nabla \rho) \end{aligned}$$

Some other applications of MGF are

$$\langle (\nabla h) e^{-iQ_z(h_1 - h_2)} \rangle = -iQ_z \nabla \rho \exp[-Q_z^2(\rho_0 - \rho)] \quad (\text{B.4a})$$

$$\langle (\nabla h A \nabla h) e^{-iQ_z(h_1 - h_2)} \rangle = \text{Trace}[A \Sigma] - Q_z^2 (\nabla \rho A \nabla \rho) \exp[-Q_z^2(\rho_0 - \rho)]. \quad (\text{B.4b})$$

In all previous equations, Σ is the covariance matrix of the slopes, $\rho = \rho(\mathbf{r})$ is the autocorrelation function of surface elevations and $\rho_0 = \rho(\mathbf{0})$.

References

- [1] Álvarez-Pérez J L 2001 An extension of the IEM/IEMM surface scattering model *Waves Random Media* **11** 307–29
- [2] Berman D H 1991 Simulations of rough surface scattering *J. Acoust. Soc. Am.* **89** 623–36
- [3] Dacol D K 1990 The Kirchhoff approximation for acoustic scattering from a rough fluid-elastic interface *J. Acoust. Soc. Am.* **88** 978–83
- [4] Dashen R and Wurmser D 1991 Applications of the new scattering formalism: the dirichlet boundary condition *J. Math. Phys.* **32** 997–1003
- [5] Dashen R and Wurmser D 1991 Approximate representations of the scattering amplitude *J. Math. Phys.* **32** 986–96
- [6] Dashen R and Wurmser D 1991 A new theory for scattering from a surface *J. Math. Phys.* **32** 971–85
- [7] Elfouhaily T, Guignard S, Awadallah R and Thompson D R 2003 Local and non-local curvature approximation: a new asymptotic theory for wave scattering *Waves Random Media* **13** 321–37
- [8] Elfouhaily T, Guignard S and Thompson D R 2003 A practical second-order electromagnetic model in the quasi-specular regime based on the curvature of a good-conducting scattering surface *Waves Random Media* **13** L1–L6
- [9] Elfouhaily T, Thompson D R, Chapron B and Vandemark D 1999 A new bistatic model for electromagnetic scattering from perfect conducting random surfaces *Waves Random Media* **9** 281–94

-
- [10] Fung A K 1994 *Microwave Scattering and Emission Model and Their Applications* (Norwood, MA: Artech House) 573 pp
 - [11] Guérin C-A and Saillard M 2003 On the high-frequency limit of the second-order small-slope approximation *Waves Random Media* **13** 75–88
 - [12] Milder D M 1991 An improved formalism for wave scattering from rough surface *J. Acoust. Soc. Am.* **89** 529–41
 - [13] Milder D M 1992 An improved formalism for wave scattering from rough surface: ii. Numerical trials in three dimensions *J. Acoust. Soc. Am.* **91** 2620–6
 - [14] Milder D M 1996 An improved formalism for electromagnetic scattering from a perfectly conducting rough surface *Radio Sci.* **31** 1369–76
 - [15] Milder D M 1998 An improved formulation of coherent forward scatter from random rough surfaces *Waves Random Media* **8** 67–78
 - [16] Rodriguez E 1989 Beyond the Kirchhoff approximation *Radio Sci.* **24** 681–93
 - [17] Smith S 1996 The operator expansion formalism for electromagnetic scattering from rough dielectric surfaces *Radio Sci.* **31** 1377–85
 - [18] Soriano G, Guérin C-A and Saillard M 2002 Scattering by two-dimensional rough surfaces: comparison between the method of moments, Kirchhoff and small-slope approximations *Waves Random Media* **12** 63–83
 - [19] Soriano G and Saillard M 2001 Scattering of electromagnetic waves from two-dimensional rough surfaces with an impedance approximation *J. Opt. Soc. Am.* **18** 124–33
 - [20] Soriano G and Saillard M 2003 Modelization of the scattering of electromagnetic waves from the ocean surface *Progress in Electromagnetic Research X* (Cambridge, Massachusetts, USA: EMW Publishing) pp 102–28
 - [21] Thorsos E and Jackson D R 1991 Studies of scattering theory using numerical methods *Waves Random Media* **3** S165–S190
 - [22] Thorsos E I 1988 The validity of the Kirchhoff approximation for rough surface scattering using a Gaussian roughness spectrum *J. Acoust. Soc. Am.* **83** 78–79
 - [23] Thorsos E I and Broshat S L 1997 An investigation of the small-slope approximation for scattering from rough surfaces: part II. Numerical studies *J. Acoust. Soc. Am.* **101** 2615–25
 - [24] Voronovich A G 1985 Small-slope approximation in wave scattering by rough surfaces *Sov. Phys.—JETP* **62** 65–70
 - [25] Voronovich A G 1994 Small-slope approximation for electromagnetic wave scattering at a rough interface of two dielectric half-spaces *Waves Random Media* **4** 337–67
 - [26] Voronovich A G 1994 *Wave Scattering from Rough Surfaces* 2nd updated edn (Heidelberg, Germany: Springer) 236 pp
 - [27] Voronovich A G 2002 The effect of modulation of bragg scattering in small-slope approximation *Waves Random Media* **1** 247–69